Chain Termination Effects of Chemically Modified Nucleoside Analogs on SARS-CoV-2 RNA Polymerase

Lin Yang[1], Xinzhou Xu[1,2], Zhibin Liang[1], Buyu Zhang[1,2], Ka Man Tse[1,2], Peter Cheung[1,2*]

1 Department of Chemical Pathology, Prince of Wales Hospital, The Chinese University of Hong Kong, Shatin, New Territories, Hong Kong SAR, China

2 Li Ka Shing Institute of Health Sciences, The Chinese University of Hong Kong, Shatin, New Territories, Hong Kong SAR, China

* Corresponding author Email: ppcheung@cuhk.edu.hk

Abstract:

In the current scenario, the available drugs for SARS-CoV-2 are extremely limited. Among the potential therapeutic targets, the RNA-dependent RNA polymerase (RdRp) complex, essential for viral replication and transcription, presents a promising focal point for drug design. This study explores the mechanistic effects of chemically modified nucleoside analogs on the activity of SARS-CoV-2 RdRp and the subsequent chain termination of viral RNA synthesis. We investigate a range of modifications, including 2'-fluoro (2'-F), 2'-O-methyl, and 3'-deoxy substitutions on the sugar as well as base component changes, to ascertain their incorporation by RdRp and resistance to proofreading by the nsp14/nsp10 exonuclease complex. Through a combination of enzymatic experiments, we elucidate the influence of these modifications on RdRp efficiency. Our findings demonstrate that 2'-OMe-NTP, 3'-dNTP, 6-Aza-UTP can enhance the likelihood of chain termination, offering insights into the design of nucleoside analogs with potent antiviral activities. The study's comprehensive analysis not only furthers our understanding of SARS-CoV-2's molecular biology but also contributes to the strategic development of antiviral agents with the potential to combat the current pandemic and prepare for future coronavirus outbreaks.

Key words: SARS-CoV-2, RNA-dependent RNA polymerase, nucleotide analog, exonuclease

1. Introduction

The emergence of SARS-CoV-2, the pathogen responsible for the COVID-19 pandemic, precipitated an urgent global health crisis of unprecedented scale. With its rapid transmission and significant mortality rates, this pandemic galvanized extensive research into the virus's molecular mechanics and potential therapeutic targets. The RNA-dependent RNA polymerase (RdRp) complex of SARS-CoV-2, which includes nonstructural proteins nsp12, nsp7, and nsp8, with nsp12 as the principal catalytic subunit, plays a critical role in the viral replication cycle (Hillen et al., 2020). This has positioned RdRp as a primary target for antiviral interventions.

Nucleoside analogs have gained prominence as antivirals by disrupting viral replication. These compounds structurally resemble the RNA's natural nucleotides, fooling RdRp into incorporating them into the viral RNA (Yang & Rao, 2021). Once embedded, they serve as chain terminators or induce mutagenesis, thus impairing the virus's replicative capabilities.

Remdesivir, for example, is an adenosine analog initially designed to tackle the Ebola virus. It contains a 1' cyano group modification on the ribose sugar, enabling it to escape excision by the viral proofreading enzymes and induce a delayed chain termination (Yin et al., 2020). Molnupiravir, or EIDD-2801, originally intended for influenza, integrates into the viral RNA as β-D-N4-hydroxycytidine, promoting a high error rate in viral genome replication—a phenomenon known as lethal mutagenesis—which compromises viral integrity (Kabinger et al., 2021).

Favipiravir, first developed to combat influenza, acts as a guanine analog. Its modified structure, featuring a furan ring and the absence of hydroxyl groups, allows for incorporation by RdRp but inhibits further RNA synthesis (Shannon et al., 2020). AT-527, explored initially for hepatitis C, has a guanosine analog backbone with a 2'-fluorine and 2'-methyl group addition, conferring resistance to proofreading and enhancing antiviral activity (Shannon et al., 2022).

Despite their ingenuity, these nucleoside analogs are not without shortcomings. The efficacy of these drugs can be compromised by their interactions with RdRp and SARS-CoV-2's sophisticated proofreading mechanisms, which can remove the incorporated analogs, undermining their therapeutic impact. For instance, Remdesivir's uptake and phosphorylation can be inefficient in certain cell types (Rasmussen et al., 2021), while Molnupiravir's mutagenic mode of action may potentially induce off-target effects, raising concerns about long-term use and viral resistance (Sanderson et al., 2023). Favipiravir requires high doses to be effective, which may not be tolerable for all patients, and its teratogenicity limits its use. The clinical efficacy of AT-527 against COVID-19 remains under investigation, with concerns about its bioavailability and metabolic stability.

Chemical modifications, such as alterations in the sugar moiety or changes in the base or phosphate groups, are strategically implemented to improve the incorporation by RdRp and to offer resistance against the exonuclease complex's proofreading activity. These modifications strive to balance effective mimicry for RdRp recognition with the robustness to resist proofreading, a key challenge in the design of nucleoside analogs (Das, Harikrishna, & Gore, 2022).

Understanding the intricate interactions between these modified nucleosides and RdRp, as well as the virus's proofreading dynamics, is critical for developing potent antiviral therapies. This encompasses exploring how RdRp complex recognizes and integrates these analogs, the resultant structural changes, and the proofreading complex's response. Our study delves into the effects of chain termination by various chemically modified nucleoside analogs on the SARS-CoV-2 RdRp, combining in vitro biochemical assays with computational modeling to discern how alterations to the ribose and base components affect their integration by RdRp and their susceptibility to proofreading. The insights gained from this investigation are poised to inform the design of new nucleoside analogs with optimized potency and proofreading resistance, propelling the development of innovative antiviral strategies against SARS-CoV-2 and future coronavirus threats.

2. Materials and Methods

2.1 Constructs, expression, and purification of the nsp12/7/8 complex (RdRp)

The nsp12/7/8 complex (RdRP) was expressed and purified in the insect cell-baculovirus system. Codon-optimized DNA sequence (BstEII-10 × His tag-nsp7-TEV site- nsp8-TEV site-nsp12-2 × strepII tag-RsrII) was chemically synthesized and cloned into the pKL-pBac backbone via BstEII and RsrII sites, initiated by a 5' ATG start codon, and flanked by two Tobacco Etch Virus (TEV) protease cleavage sites for post-translational processing. The baculovirus coding for the nsp complex was generated by transfecting the bacmid into Expi-Sf9 cells as P0 virus. P1 virus was amplified by infecting 50 ml fresh Sf9 cells at a density of 2×10^6/mL with 1 mL P0 virus. After 5 to 7 days, the clarified culture medium was filtered and supplemented with 0.5% BSA and stored at 4°C protected from light.

Expression of the recombinant proteins was carried out in High Five cells, cultured in ESF 921 serum-free medium (Expression Systems) at 27 °C. At a density of 2-3 million cells per mL, 200 mL of High Five cells was infected with 10 mL P1 virus for 3 to 5 days. The cells were harvested by centrifugation at 500 × g for 5 min, and the resultant cell pellets were promptly frozen and preserved at −80 °C for further analysis.

The insect cells pellets harboring the co-expressed RdRp complex were resuspended in a binding buffer composed of 50 mM HEPES (pH 7.4), 250 mM NaCl, 5 mM $MgCl_2$, 1 mM dithiothreitol (DTT), and 10% (v/v) glycerol, supplemented with an EDTA-free Protease Inhibitor Cocktail (TargetMol). Cell lysis was performed using a high-pressure homogenizer set to 500 bar. The insoluble material was removed by centrifugation at 40,000 rpm (Eppendorf himac CP100NX) for 30 min at 4 ℃, and further removed by passage through 0.45 μm filter.

Strep-Tactin®XT 4Flow® 50% suspension (IBA Lifescience) was washed with 10 volumes wash buffer and added into column. The clear supernatant from last step was added into column in flow-through mode. Then the beads were washed by 10 column

volume of wash buffer (50 mM HEPES (pH 7.4), 250 mM NaCl, 5 mM $MgCl_2$, 1 mM dithiothreitol (DTT), and 10% (v/v) glycerol) and eluted with 10 column volume of elution buffer (50 mM HEPES (pH 7.4), 250 mM NaCl, 5 mM $MgCl_2$, 1 mM dithiothreitol (DTT), and 10% (v/v) glycerol, 100 mM biotin, 2 mM EDTA).buffer exchange

2.2 Constructs, expression, and purification of the nsp14/10 complex

The nsp14/10 complex was expressed and purified in the insect cell-baculovirus system. Codon-optimized DNA sequence (BstEII-10xHis tag-nsp14- TEV site-nsp10-2xstrepII tag-RsrII) was synthesized and cloned into the pKL-pBac backbone via BstEII and RsrII sites. The expression and purification cleavage were conducted as described in *Constructs, expression, and purification of the nsp12/7/8 complex (RdRp)* with minor modifications.

The baculovirus coding for the nsp complex was generated by transfecting the bacmid into Expi-Sf9 cells as P0 virus. P1 virus was amplified by infecting 50 ml fresh Sf9 cells at a density of 2×10^6/mL with 1 mL P0 virus. After 5 to 7 days, the clarified culture medium was filtered and supplemented with 0.5% BSA and stored at 4°C protected from light.

Expression of the recombinant proteins was carried out in High Five cells, cultured in ESF 921 serum-free medium (Expression Systems) at 27 °C. At a density of 2-3 million cells per mL, 200 mL of High Five cells was infected with 10 mL P1 virus for 3 to 5 days. The cells were harvested by centrifugation at 500 × g for 5 min, and the resultant cell pellets were promptly frozen and preserved at −80 °C for further analysis.

The insect cells pellets harboring the co-expressed nsp14/10 complex were resuspended in a binding buffer composed of 50 mM HEPES (pH 7.4), 250 mM NaCl, 5 mM $MgCl_2$, 1 mM dithiothreitol (DTT), and 10% (v/v) glycerol, supplemented with an EDTA-free Protease Inhibitor Cocktail (TargetMol). Cell lysis was performed using a high-pressure homogenizer set to 500 bar. The insoluble material was removed by centrifugation at 40,000 rpm (Eppendorf himac CP100NX) for 30 min at 4 ℃, and further removed by passage through 0.45 μm filter.

BeyoGold™ His-tag Purification Resin (Beyotime) was washed with 10 volumes wash buffer and added into column. 200 mL cell lysate was added into column in flow-through mode. Then the beads were washed by 510 column volume of wash buffer (50 mM HEPES (pH 7.4), 250 mM NaCl, 5 mM $MgCl_2$, 1 mM dithiothreitol (DTT), and 10% (v/v) glycerol) and eluted with 10 column volume of elution buffer (50 mM HEPES (pH 7.4), 250 mM NaCl, 5 mM $MgCl_2$, 1 mM dithiothreitol (DTT), and 10% (v/v) glycerol, 250 mM imidazole). The eluted buffer was further purified with Streptavidin beads as below.

Strep-Tactin®XT 4Flow® 50% suspension (IBA Lifescience) was washed with 10 volumes wash buffer and added into column. Eluted buffer from Ni-NTA resin purification was added into column in flow-through mode. Then the beads were washed by 10 column volume of wash buffer (50 mM HEPES (pH 7.4), 250 mM NaCl, 5 mM $MgCl_2$, 1 mM dithiothreitol (DTT), and 10% (v/v) glycerol) and eluted with 10 column volume of elution buffer (50 mM HEPES (pH 7.4), 250 mM NaCl, 5 mM $MgCl_2$, 1 mM dithiothreitol (DTT), and 10% (v/v) glycerol, 100 mM biotin, 2 mM EDTA).buffer exchange

2.3 RdRp Enzymatic Activity Assay and Its Inhibition by Nucleotide Analogues

In this assay, a fluorescence-labeled short RNA oligonucleotide, referred to as LS2U, with the sequence 5'-FAM-GUCAUUCUCCUAAGAAGCUU-3', was used as the primer strand. For the template strand, a longer RNA oligonucleotide named LS15A, with the sequence 5'-CUAUCCCCAUGUGAUUUUACAAGCUUCUUAGGAGAAUGAC-3', was employed. The SARS-CoV-2 RdRp (RNA-dependent RNA polymerase) complex, purified from insect cells, was utilized at a final concentration of 1 μM. The RdRp complex was incubated with 0.1 μM of the double-stranded RNA and 100 μM of rNTPs (ribonucleoside triphosphates) in a reaction buffer. This buffer included 1.14 U/μl RNase inhibitor and was composed of 20 mM Tris (pH 7.5), 15 mM NaCl, and 5 mM $MgCl_2$. All components were prepared with RNase-free water to ensure the purity of the reaction. The total volume of the reaction mixture was maintained at 10 μL.

After a 10-minute incubation period at 37°C, a 4 μL aliquot of the reaction mixture was combined with 4 μL of 2x RNA loading buffer, which included formamide and EDTA. The combined sample (8 μL in total) was then loaded onto a 10% Urea-PAGE gel for denaturation analysis. Electrophoresis was conducted at 300V for 20 minutes, followed by imaging with a LI-COR Odyssey M Imager.

The procedure for evaluating the inhibition of the RdRp enzymatic activity by nucleotide analogues was essentially identical to the RdRp enzymatic assay described above. However, in the inhibition assays, each nucleotide analogue was introduced at a final concentration of 100 μM, replacing the corresponding NTP.

2.4 Exonuclease Activity Assays with Nucleotide Analogue Substitution

The 5′-fluorescein-labeled oligonucleotide, LS2U, previously mentioned in the RdRp Enzymatic Activity Assay, was prepared at a concentration of 0.1 μM. It was combined with an equimolar amount of the complementary strand, LS15A-RNA. This duplex was then introduced into a reaction buffer composed of 20 mM Tris (pH 7.5) and 5 mM MgCl2. The enzymatic reaction was initiated by the addition of 1 μM of the SARS-CoV-2 RdRp (RNA-dependent RNA polymerase) complex and a rNTP mix at a concentration of 100 μM, with each nucleotide analogue substituting for the corresponding rNTP. The mixture was incubated at 37°C for 10 minutes to form stalled RNA products. This was followed by the addition of a series of dilutions of the nsp14–nsp10 complex, with a further incubation at 37°C for an additional 10 minutes. The reactions were halted by the introduction of 2x RNA loading buffer. The resulting reaction products were resolved on a 10% TB-Urea polyacrylamide gel and were visualized using a LI-COR Odyssey M Imager.

3. Results

3.1 Impact of Nucleoside Analogs on SARS-CoV-2 RNA Polymerase Activity

In exploring the potential antiviral mechanisms against SARS-CoV-2, we investigated the effects of various chemically modified nucleoside analogs on the activity of the RNA-dependent RNA polymerase (RdRp). The modifications of these analogs are designed to interfere with the natural RNA synthesis process. 2’OMe-GTP, 2’OMe-UTP, 2’OMe-ATP and 2’OMe-CTP modified with a 2'-O-methyl group on the ribose sugar, resulted in immediate termination of RNA synthesis upon integration into the growing RNA chain, evident from the truncated products observed during gel electrophoresis (Figure 1B). 3’-dGTP, 3’-dUTP, 3’-dATP and 3’-dCTP lacking the crucial 3'-hydroxyl group necessary for phosphodiester bond formation, similarly led to immediate chain termination, underscoring their robust inhibitory effect on RdRp activity (Figure 1B). The addition of 5’-Methyl-3’-dUTP, which bears a methyl group at the 5’ position of the uracil base and is also devoid of the 3'-hydroxyl group, consistently terminated RNA elongation immediately, further validating the termination effect of 3'-hydroxyl absence (Figure 1B). In contrast, 6-Aza-UTP, with a nitrogen atom replacing carbon at the 6-position of uracil, acted as a delayed chain terminator. The polymerase extended several nucleotides past the incorporation point of this analog before halting, indicating a disruption to the enzyme's processivity that is not immediately detrimental (Figure 1B). The 2’-F-dGTP, 2’-F-dUTP, 2’-F-dATP and 2’-F-dCTP contain a fluorine atom at the 2’ position of the ribose, which, however, did not disrupt the elongation process post-incorporation, suggesting that this modification cannot be utilized in therapeutic designs where complete chain termination is desired (Figure 1B). Conversely, 3’-(O-Propargyl)-GTP, with a propargyl group linked to the 3’ oxygen of the ribose, showed no incorporation, suggesting a possible steric or chemical incompatibility with the RdRp, leading to a non-productive enzyme-nucleotide complex (Figure 1B). These diverse effects—from immediate to delayed termination, as well as complete non-incorporation—illustrate the range of potential interactions between RdRp and modified nucleoside analogs. The termination patterns of these analogs highlight their promise for the development of targeted antiviral therapies, leveraging their structural modifications to disrupt the viral replication machinery.

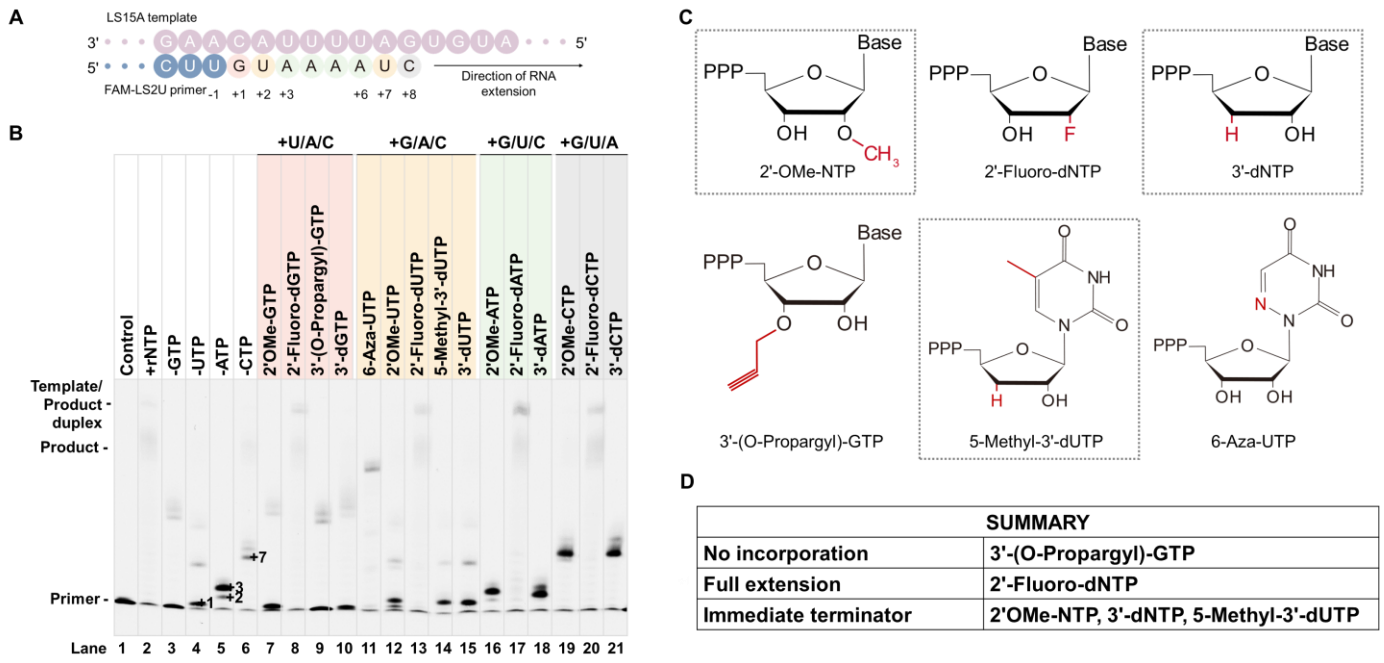

SUMMARY	
No incorporation	3'-(O-Propargyl)-GTP
Full extension	2'-Fluoro-dNTP
Immediate terminator	2'OMe-NTP, 3'-dNTP, 5-Methyl-3'-dUTP

Figure 1. Evaluation of applicability of NuA as chain terminator on SARS-CoV-2 RdRP. (A) LS15A RNA template and LS2U RNA primer scaffolds used for RNA extension Assay (Moeller et al., 2022). The LS15A RNA template contains 40 nucleotides, and the LS2U RNA primer contains 20 nucleotides, fluorescently labelled 5′ overhang. **(B)** Incubation of the RdRp complex with LS15A-LS2U RNA duplex and each nucleotide analogue leads to efficient RNA extension, termination, or no incorporation. **(C)** Chemical structures of the natural NTPs and NuAs employed in this study.

3.2 Resistance of RdRp Inhibitors to nsp14/nsp10 Exoribonuclease Activity

The proofreading ability of SARS-CoV-2 poses a challenge for the development of nucleoside analogue-based antiviral drugs. Hence, subsequent experiments were designed to evaluate the resistance of RdRp-inhibiting nucleoside analogs to the exonucleolytic proofreading by the nsp14/nsp10 complex of SARS-CoV-2. Among the analogs tested in Figure 1B, only the RNA chains terminated by 3'-dNTP exhibited a notable resistance to nsp14/nsp10 activity, suggesting that the lack of a 3' hydroxyl group may confer some protective effect against exonuclease-mediated degradation, which is consistent with previous work(Liu et al., 2021). Conversely, terminated products resulting from incorporation of 2'OMe-NTP, 5'-Methyl-3'-dUTP, and 6-Aza-UTP did not display significant resistance and were susceptible to cleavage by the nsp14/nsp10 complex, as indicated by the reduction of terminated RNA products in gel electrophoresis (Figure 2). These findings highlight the unique potential of 3'-deoxy NuAs for developing antiviral strategies that could bypass the viral proofreading mechanism, which is critical for the fidelity of viral replication.

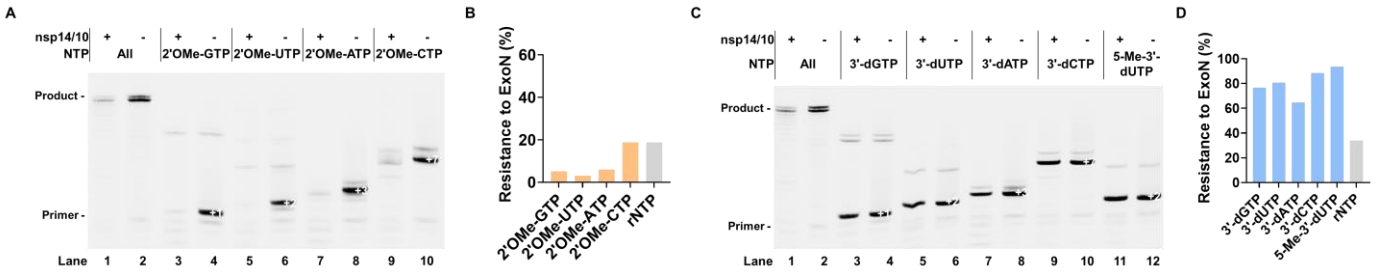

Figure 2. Assessing ExoN resistance with an extension-cleavage assay. (A) Cleavage of RNA substrates incorporating 2'-O-methylated ribonucleotides by the SARS-CoV-2 nsp14/nsp10 complex. **(B)** Quantification of No Cleavage Rate (ExoN resistance) in Panel A. **(C)** Cleavage of RNA substrates containing 2'-deoxyribonucleotides by the SARS-CoV-2 nsp14/nsp10 complex. **(D)** Quantification of No Cleavage Rate (ExoN resistance) in Panel C.

4. Discussion

Author contributions

Acknowledgments

Conflicts of Interest

Data Availability Statement

5. Reference

Das, G., Harikrishna, S., & Gore, K. R. (2022). Influence of Sugar Modifications on the Nucleoside Conformation and Oligonucleotide Stability: A Critical Review. *Chem Rec, 22*(12), e202200174. doi:10.1002/tcr.202200174

Hillen, H. S., Kokic, G., Farnung, L., Dienemann, C., Tegunov, D., & Cramer, P. (2020). Structure of replicating SARS-CoV-2 polymerase. *Nature, 584*(7819), 154-156. doi:10.1038/s41586-020-2368-8

Kabinger, F., Stiller, C., Schmitzova, J., Dienemann, C., Kokic, G., Hillen, H. S., . . . Cramer, P. (2021). Mechanism of molnupiravir-induced SARS-CoV-2 mutagenesis. *Nat Struct Mol Biol, 28*(9), 740-746. doi:10.1038/s41594-021-00651-0

Liu, C., Shi, W., Becker, S. T., Schatz, D. G., Liu, B., & Yang, Y. (2021). Structural basis of mismatch recognition by a SARS-CoV-2 proofreading enzyme. *Science, 373*(6559), 1142-1146. doi:10.1126/science.abi9310

Moeller, N. H., Shi, K., Demir, O., Belica, C., Banerjee, S., Yin, L., . . . Aihara, H. (2022). Structure and dynamics of SARS-CoV-2 proofreading exoribonuclease ExoN. *Proc Natl Acad Sci U S A, 119*(9). doi:10.1073/pnas.2106379119

Rasmussen, H. B., Jurgens, G., Thomsen, R., Taboureau, O., Zeth, K., Hansen, P. E., & Hansen, P. R. (2021). Cellular Uptake and Intracellular Phosphorylation of GS-441524: Implications for Its Effectiveness against COVID-19. *Viruses, 13*(7). doi:10.3390/v13071369

Sanderson, T., Hisner, R., Donovan-Banfield, I., Hartman, H., Lochen, A., Peacock, T. P., & Ruis, C. (2023). A molnupiravir-associated mutational signature in global SARS-CoV-2 genomes. *Nature, 623*(7987), 594-600. doi:10.1038/s41586-023-06649-6

Shannon, A., Fattorini, V., Sama, B., Selisko, B., Feracci, M., Falcou, C., . . . Canard, B. (2022). A dual mechanism of action of AT-527 against SARS-CoV-2 polymerase. *Nat Commun, 13*(1), 621. doi:10.1038/s41467-022-28113-1

Shannon, A., Selisko, B., Le, N. T., Huchting, J., Touret, F., Piorkowski, G., . . . Canard, B. (2020). Rapid incorporation of Favipiravir by the fast and permissive viral RNA polymerase complex results in SARS-CoV-2 lethal mutagenesis. *Nat Commun, 11*(1), 4682. doi:10.1038/s41467-020-18463-z

Yang, H., & Rao, Z. (2021). Structural biology of SARS-CoV-2 and implications for therapeutic development. *Nat Rev Microbiol, 19*(11), 685-700. doi:10.1038/s41579-021-00630-8

Yin, W., Mao, C., Luan, X., Shen, D. D., Shen, Q., Su, H., . . . Xu, H. E. (2020). Structural basis for inhibition of the RNA-dependent RNA polymerase from SARS-CoV-2 by remdesivir. *Science, 368*(6498), 1499-1504. doi:10.1126/science.abc1560